Photoacoustic Based Visual Servoing of Needle Tips to Improve Biopsy on Obese Patients

Joshua Shubert* Muyinatu A. Lediju Bell*†
*Department of Electrical and Computer Engineering, Johns Hopkins University, Baltimore, MD, USA
†Department of Biomedical Engineering, Johns Hopkins University, Baltimore, MD, USA

***Abstract*—For many routine surgeries and procedures, such as liver biopsies, obese patients present an increased challenge. In liver biopsies, it is more difficult to visualize the needle tip in real-time abdominal ultrasound images, particularly when multiple layers of fat and other tissues obscure needle localization, which results in multiple needle passes to obtain an adequate biopsy sample. This work aims to develop a robotic system that can autonomously and robustly follow a biopsy needle regardless of the tissue medium by using photoacoustic imaging. Our system consists of a robotically controlled ultrasound probe that continually visualizes the location of the biopsy needle tip by segmenting photoacoustic signals generated from an optical fiber inside the needle. This system was able to track and remain centered over a needle inserted in fat, muscle, and liver tissue with mean errors of less than 1mm, and it successfully recovered from a perturbation of the ultrasound transducer that caused the needle to exit the image plane. Our results show promise for guiding biopsies in obese patients with this novel system.**

***Index Terms*—photoacoustics, robotics, visual servoing, biopsy**

I. Introduction

Approximately 37.7% of adults in the United States are obese, which is an increase of 30% since the 1980s [1], [2]. This growing trend requires old procedures to be adapted and new procedures to be developed to meet the needs of this patient demographic. For example, the most common form of liver biopsy is percutaneous liver biopsy, where a needle is inserted into the liver through the abdomen, which is frequently performed under ultrasound image guidance. Obese patients are considered to be high-risk patients for percutaneous liver biopsy as it is more difficult to visualize the needle, which results in multiple needle passes to obtain an adequate biopsy sample and increases the risk of complications from 4% up to 14%. The most serious complication associated with multiple needle passes is intraperitoneal hemorrhaging [3] [4]. Laparoscopic biopsy is one alternative to percutaneous biopsy but it is more invasive, often requiring general anesthesia, and it is generally not performed on obese patients [5]. Transjugular liver biopsy is an alternative for obese patients, but it requires the use of fluoroscopic guidance and contrast agents which can be harmful and are not suitable for patients who have allergic reactions to these contrast agents [6].

We propose a new method for performing percutaneous liver biopsy that involves the combination of photoacoustic imaging to improve the visualization of the biopsy needle tip in obese patients and a servoing robot to maintain sight of the needle tip at all times. Photoacoustic imaging uses laser light of specific wavelengths to generate acoustic signals that can be detected with conventional ultrasound transducers [7]. This photoacoustic effect can be used to induce the generation of acoustic signals at the tip of the biopsy needle when an optical fiber is inserted into the needle and the other end of the fiber is coupled to a pulsed laser source [8]. The resulting photoacoustic images enable visualization and localization of the needle tip when it is in the image plane.

While several ultrasound guided robotic biopsy systems already exist [9]–[11], the use of traditional ultrasound imaging for visual servoing is not suitable for obese patients because increased signal attenuation and acoustic clutter complicate needle tip localization. By combining the localized signal generation of photoacoustic imaging and the hands-free visualization provided by a robotic assistant, we propose and investigate a novel biopsy approach to provide obese patients with an improved level of care.

II. System Overview

The general workflow of our robotic biopsy needle tracking system is shown in Figure 1. The core components are a 1064 nm pulsed Nd:YAG laser, an E-CUBE 12R ultrasound scanner (Alpinion Medical Systems), and a Sawyer robot (Rethink Robotics). A custom end effector was created to allow Sawyer to hold an Alpinion L3-8 linear array ultrasound transducer. This probe was then calibrated using the method described by Kim et al [12]. The needle tracking system requires that

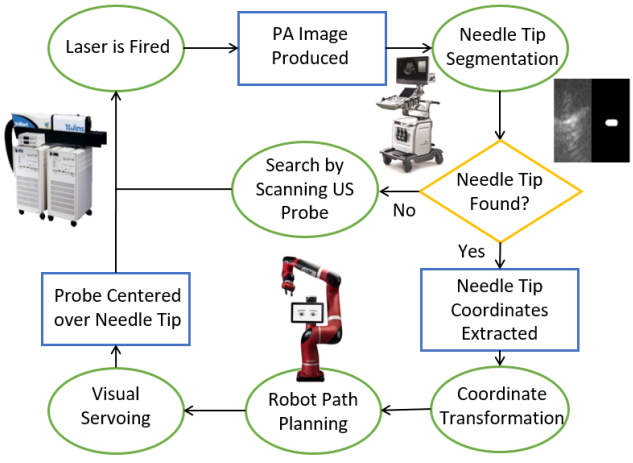

Fig. 1: System Diagram

the biopsy needle for the procedure have an optical fiber inserted, and that the fiber is coupled to a laser source. Then, the ultrasound probe held by Sawyer is placed onto the patient's surface and visual servoing is activated. The visual servoing system consists of two main components: (1) needle tip segmentation and (2) probe centering.

A. Needle Tip Segmentation

Needle tip segmentation was performed using a sequence of image processing steps. First, binary thresholding was applied to the photoacoustic image. The threshold was dynamically selected based on the maximum intensity in the image frame. Second, binary erosion and dilation was performed to remove single pixel regions and increase performance of the next step: connected component labeling. The pixel area was calculated for each label and the frequency of each area measurement was displayed as a histogram. The needle tip label was selected as the label with largest area, only if the magnitude of this area was also an outlier in the histogram. If there was no distinct outlier, the algorithm assumed that the needle tip was not visible in the image frame. If an outlier existed, the needle tip location for that frame was calculated as the centroid of the labeled region. For robustness, the segmentation results from 5 previous frames were compared for spatiotemporal continuity before reporting the final decision. If there were 5 consecutive failures to find the needle tip in the photoacoustic image, the Sawyer robot scanned back and forth. At each step of the scanning, the image was segmented to locate the needle tip. If the needle tip was located, the scanning stopped. Otherwise, the scanning continued until a user-defined timeout.

B. Probe Centering

If the needle tip locations, p, in each frame were spatially consistent, they were averaged together to produce the most likely location of the needle tip, $\bar{p}$. The vector, p_{center}, was then computed as the vector from the center of the top row of the image to $\bar{p}$. The x component of this vector, $\bar{p}_{center,x}$, was then mapped into robot coordinates according to (1), where F_{cal} is the transformation obtained from calibrating the ultrasound probe and F_{robot} is the frame transformation from Sawyer's end-effector to Sawyer's base.

$$p_{robot} = F_{robot} F_{cal} \bar{p}_{center,x} \tag{1}$$

Sawyer then computes a trajectory to minimize p_{robot}, which will result in the ultrasound probe being centered over $\bar{p}$.

III. Methods

Experiments were developed to evaluate three aspects of the system: (1) segmentation validation experiment to determine how well the segmentation algorithm finds and tracks the needle tip, (2) ultrasound probe centering experiment to determine how well the robot centers the probe on the segmented needle tip, and a (3) perturbation recovery experiment to determine how well the system recovers from real world disruptions and out-of-plane motion.

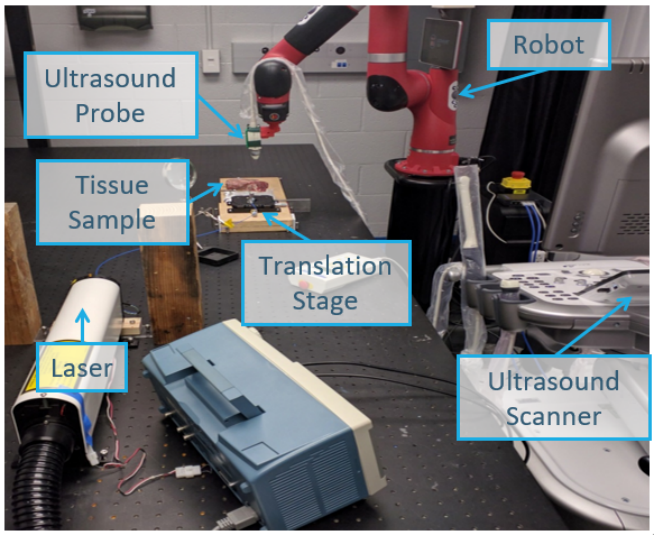

Fig. 2: Experimental Setup

A. Segmentation Validation Experiment

A needle (representing a biopsy needle) was fixed to a manual translation stage, a 1 mm diameter optical fiber was inserted through the hollow core of the needle, and the tip of the fiber was fixed at the tip of this needle. This fiber-needle pair was then inserted 10 times into each of the three tissue samples: *ex vivo* chicken breast (representing fat), *ex vivo* sirloin steak meat from the back of a cow (representing muscle), and *ex vivo* sheep liver. Water was used as a control to obtain best-case results in the presence of possible needle tip deflections, optical and acoustic scattering, and acoustic clutter. A photograph of the experimental set-up is shown in Figure 2.

After the initial insertion, the ultrasound probe was positioned to visualize the needle tip in the photoacoustic image with the lateral axis of the ultrasound probe parallel to the needle. After this alignment was completed, the location, p_a, of the needle tip was segmented and the needle was advanced using the manual translation stage. The new location, p_b, of the needle tip was then segmented from the photoacoustic image after the insertion was completed. The system was evaluated by comparing the difference between these two needle locations in the photoacoustic image ($p_b - p_a$) and the ground truth distance, d_n, obtained from the translation stage readings, as illustrated in Figure 3.

B. Probe Centering Experiment

The same set-up described in Section III-A was used for the probe centering experiment, with the exception that the needle was stationary and robotic ultrasound probe movement was added. For each of 10 trials, the probe was first manually placed so that the needle tip was visible but not yet centered in the image. The visual servoing software was activated and the robot moved the probe so that it became centered over the needle tip signal. The system was evaluated by measuring the distance d_p (in image coordinates) between the photoacoustic signal and the center of the ultrasound probe after the robot stopped moving, as illustrated in in Figure 4.

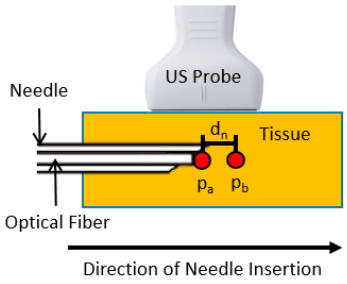

Fig. 3: Segmentation Validation Experiment

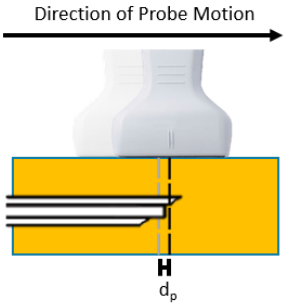

Fig. 4: Probe Centering Experiment

C. Perturbation Recovery and Out-of-Plane Motion Experiment

The needle was fixed to the manual translation stage and then rotated from +20 to -20 degrees, in 10-degree increments, relative to the lateral axis of the ultrasound probe. Needle insertions into the liver sample were performed with these five insertion angles. The needle was continuously advanced into the liver sample a total distance of 13 mm while the robotic system segmented the needle tip location and moved the ultrasound probe to a centered position over the needle tip during this motion. If the needle tip moved out of the imaging plane of the ultrasound probe, the robotic system scanned back and forth over a distance of 60 mm in attempts to recover sight of the needle tip. If the robot found the signal it stopped scanning and returned to centering itself over the needle tip. Otherwise, the trial was considered a failure and the system would cease visual servoing.

These angled insertions were repeated with the addition of manual perturbation of the ultrasound probe, which were representative of a clinician switching to ultrasound imaging to confirm a biopsy target midway through visual servoing. The ultrasound probe was intermittently pulled away from the needle tip (utilizing cooperative control of the ultrasound probe [13]), causing the probe to lose sight of the photoacoustic signal. Then, the robotic system scanned with the ultrasound probe in attempts to recover sight of the needle tip and continue visual servoing.

IV. Results and Discussion

A. Needle Tracking

The results of the needle tracking validation experiment are shown in Figure 5. The mean tracking errors from 10 trials were 1.64, 0.57, 1.37, and 0.61 mm in fat, muscle, liver, and water, respectively. Representative photoacoustic images of the needle tip in each tissue type and in water are shown in Figure 6.

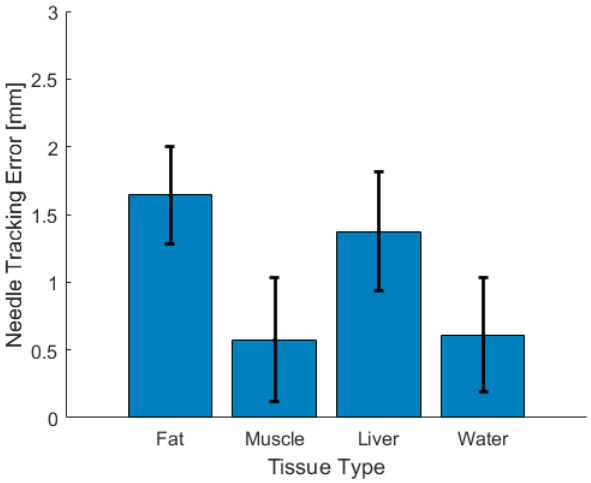

Fig. 5: Needle Tracking Results

B. Probe Centering

The results of the probe centering experiment are shown in Figure 7. The mean centering error from 10 trials is below 1 mm for three tissue types and the control (water) with liver having the highest mean error at 0.89 mm and fat having the lowest mean error at 0.45 mm. The lower bound on probe centering error is determined by the physical limits of the robot and its ability to make submillimeter corrections, thus it is not surprising that errors are more consistent for the different tissue samples when compared to the previous experiment. For the water trial, a portion of needle shaft was present in

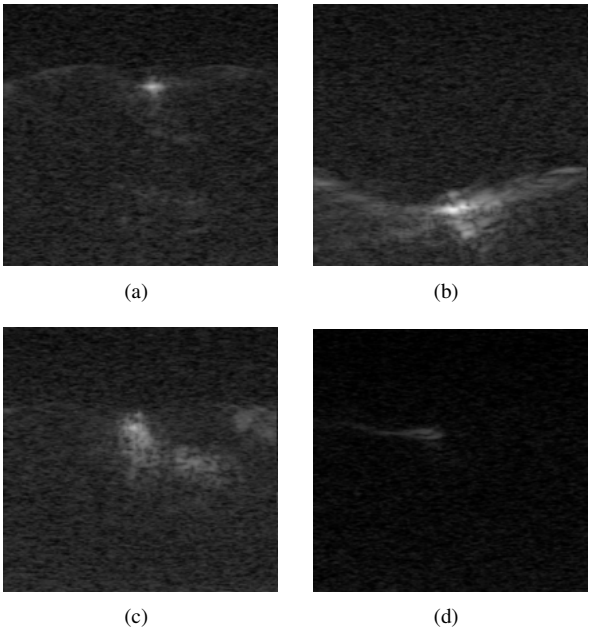

Fig. 6: Representative photoacoustic images (35 mm width x 30 mm depth) of the needle tip in (a) fat (b) liver (c) muscle (d) water.

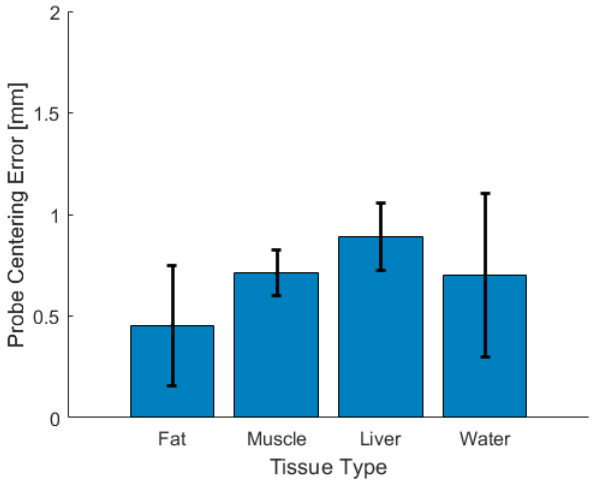

Fig. 7: Probe Centering Results

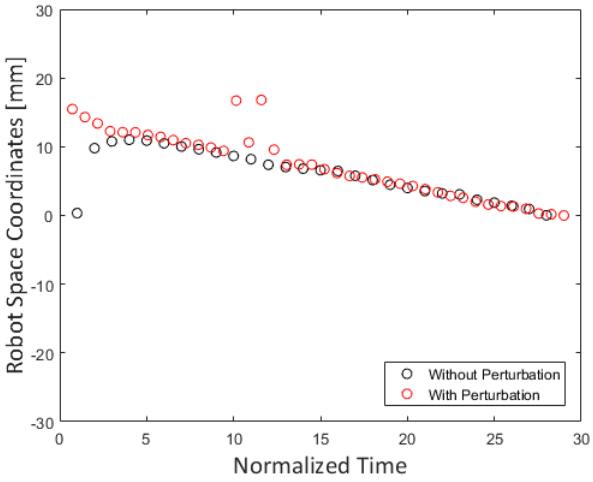

Fig. 8: Perturbation Recovery Results

the photoacoustic image (as shown in Figure 6(d)), which decreased the centering accuracy.

C. Angled Approach and Perturbation Recovery

The system maintained continuous visualization of the needle tip in 100% of the 10 trials. For the trials without perturbation the mean centering error was 0.76 mm with one standard deviation of 0.25 mm. For the trials with perturbation the mean centering error was 0.84 mm with one standard deviation of 0.47 mm. Figure 8 shows the trajectories of the ultrasound probe for two trials performed with the needle inserted at the same angle, with and without perturbation. These results demonstrate that the proposed system can recover sight of the needle tip and center it in the photoacoustic image.

The results of these experiments highlight the ability of our robotic system to track photoacoustic signals from biopsy needle tips with high accuracy regardless of the tissue medium, indicating strong potential for this system to assist with performing percutaneous biopsies on obese patients. This observation is particularly true if the photoacoustic signal is used in combination with ultrasound imaging performed with an alternative beamformer that is tailored for obese patients, such as Short-Lag Spatial Coherence [14].

V. Conclusion

This work demonstrates the first implementation of visual servoing using photoacoustic imaging. Our system maintained visualization of a needle tip by centering the ultrasound probe over the needle tip with sub-millimeter accuracy. In addition, the system recovered visualization of the needle tip after perturbations caused the system to lose sight of the needle tip. These results demonstrate the promise of such a system to assist with biopsies on obese patients or in other scenarios where traditional ultrasound guidance is inadequate. Although this work focuses on exploring the feasibility for liver biopsies (and includes the various tissues encountered when accessing the liver percutaneously), this system could be reasonably extended and adapted to other types of biopsies such as kidney or breast biopsies. A similar system could also be implemented for catheter tracking rather than needle tracking.

Acknowledgment

This work is supported by the National Science Foundation Graduate Research Fellowship awarded to Joshua Shubert and was partially funded by NIH R00 EB018994.

References

[1] K. Flegal, D. Kruszon-Moran, M. Carroll, C. Fryar, and C. Ogden. "Trends in obesity among adults in the United States, 2005 to 2014." Jama 315, no. 21 (2016): 2284-2291.

[2] Marie Ng et al. "Global, regional, and national prevalence of overweight and obesity in children and adults during 19802013: a systematic analysis for the Global Burden of Disease Study 2013." The lancet 384, no. 9945 (2014): 766-781.

[3] J. Perrault, D. McGill, B. Ott, and W. Taylor. "Liver biopsy: complications in 1000 inpatients and outpatients." Gastroenterology 74, no. 1 (1978): 103-106.

[4] F. Piccinino, E. Sagnelli, G. Pasquale. "Complications following percutaneous liver biopsy. A multicentre retrospective study on 68,276 biopsies" Journal of Hepatology 2, no. 2 (1986), 165-173.

[5] A. Bravo, S. Sheth, and S. Chopra. "Liver Biopsy" New England Journal of Medicine 344, (2001): 495-500.

[6] M. Ble et al. "Transjugular liver biopsy." Clinics in liver disease 18.4 (2014): 767-778.

[7] Bouchard, Richard, Onur Sahin, and Stanislav Emelianov. "Ultrasound-guided photoacoustic imaging: current state and future development." IEEE transactions on ultrasonics, ferroelectrics, and frequency control 61, no. 3 (2014): 450-466.

[8] Piras, Daniele, et al. "Photoacoustic needle: minimally invasive guidance to biopsy." Journal of biomedical optics 18.7 (2013): 070502-070502.

[9] M. Vitrani, G. Morel, and T. Ortmaier. "Automatic guidance of a surgical instrument with ultrasound based visual servoing." In Robotics and Automation, 2005. ICRA 2005. Proceedings of the 2005 IEEE International Conference on, pp. 508-513. IEEE, 2005. Harvard

[10] M. Sauve, P. Poignet, and E. Dombre. "Ultrasound image-based visual servoing of a surgical instrument through nonlinear model predictive control." The International Journal of Robotics Research 27, no. 1 (2008): 25-40.

[11] Kettenbach, Joachim, et al. "Robot-assisted biopsy using ultrasound guidance: initial results from in vitro tests." European radiology 15.4 (2005): 765-771.

[12] C. Kim et al. "Ultrasound probe and needle-guide calibration for robotic ultrasound scanning and needle targeting." IEEE Transactions on Biomedical Engineering 60.6 (2013): 1728-1734.

[13] Sen, H. Tutkun, et al. "A cooperatively controlled robot for ultrasound monitoring of radiation therapy." Intelligent Robots and Systems (IROS), 2013 IEEE/RSJ International Conference on. IEEE, 2013.

[14] M. Lediju et al. "Short-lag spatial coherence of backscattered echoes: Imaging characteristics." IEEE transactions on ultrasonics, ferroelectrics, and frequency control 58.7 (2011).